

Soft X-ray Femtosecond Coherent Synchrotron Radiation in a Storage Ring

C. Evain, M.E. Couprie, A. Nadji, A. Loulergue, and J.M. Filhol

*Synchrotron SOLEIL, Saint Aubin, BP 34, 91192 Gif-sur-Yvette, France*

A.A. Zholents

*Advanced Photon Source, Argonne National Laboratory, Argonne, IL 60439*

(November 19, 2010)

To be published by the American Physical Society in *Physical Review Letters*.

# Soft X-ray Femtosecond Coherent Synchrotron Radiation in a Storage Ring

C. Evain, M.E. Couprie, A. Nadji, A. Loulergue, and J.M. Filhol  
*Synchrotron SOLEIL, Saint Aubin, BP 34, 91192 Gif-sur-Yvette, France.*

A.A. Zholents

*Advanced Photon Source, Argonne National Laboratory, Argonne, Illinois 60439, USA.*

(Dated: November 19, 2010)

We propose to produce femtosecond pulses of soft x-ray coherent synchrotron radiation in a storage ring for user pump-probe experiments using two energy exchanges between a picosecond relativistic electron bunch and two external ultra-short laser pulses. The coherent emission is generated thanks to the two laser/electron interactions that modulate the longitudinal charge distribution of the electron bunch at a harmonic of the laser wavelength, such as in the echo-enabled harmonic generation in free electron lasers. Application to the SOLEIL storage ring in the soft x-ray range leads to coherent radiation and improvement of the flux of the photons by several orders in magnitude compared to the conventional slicing scheme. This is also accompanied by a significant improvement in the signal-to-noise ratio.

PACS numbers: 05.45.-a, 42.65.Sf, 41.60.Cr

With the recent advance of femtosecond (fs) spectroscopy [1], observing out-of-equilibrium molecular motion, disordered media and distorted crystal lattices in real time became possible. In the usual pump-probe technique, the pump (an ultra-short laser) creates a wave packet, the evolution of which reflects that of the ensemble of excited molecules, that is probed by a second ultra-short laser pulse providing a spectroscopic signature that is further converted into structural dynamics. Extending the studies from diatomic molecules to larger and more complex systems encounters some ambiguity with the conversion of the spectroscopic to structural information, requiring the use of an ultra-fast x-ray probe with techniques such as diffraction for crystal [2–5] or x-ray absorption spectroscopy for dilute and amorphous systems [6–10]. For revealing the structural dynamic in real time on an atomic time scale, intense stable fs x-ray sources are required. One can select from among laboratory sources either high-order harmonic generation from an intense laser focused in a rare gas [11], still limited to the order of 1 keV [12], or laser-generated plasma sources resulting from the emission of an intense laser beam onto a metal or liquid target [13], still with a rather low intensity at a high repetition rate [14]. Storage ring based synchrotron light sources [15] provide tunable high brilliance x-ray pulses thanks to very small electron beam emittance (i.e., small values of horizontal and vertical RMS beam sizes  $\sigma_x$ ,  $\sigma_y$  and divergences  $\sigma_{x'}$ ,  $\sigma_{y'}$ ). Typical pulse length is directly linked to the electron bunch length  $\sigma_z$  and is approximately tens of picoseconds long. The so-called "slicing" technique [16], which is currently under operation at ALS [17], BESSY [18], SLS [19] and is under preparation at SOLEIL [20], can produce subpicosecond synchrotron radiation pulses. In this scheme, a resonant interaction of an electron beam with an external intense ultra-short laser pulse in a tuned undulator induces an energy modulation of the electron bunch that is several times larger than the RMS beam energy spread  $\sigma_E$ . This energy modulation is transformed into modulation of an electron transverse coordinate or angle with

an amplitude much larger than correspondent beam sizes ( $\sigma_x$ ,  $\sigma_{x'}$ ), and finally the radiation can be collected separately, giving synchrotron radiation with approximately the same duration as the duration of the laser pulse. As only a fraction of the electrons participates in the subpicosecond synchrotron radiation, the peak flux of photons is reduced by approximately a factor of 10. Moreover, the total number of photons in a subpicosecond pulse is reduced proportionally to the pulse length, and the repetition rate of the subpicosecond pulses is defined by the one of the laser, which is significantly smaller than the bunch repetition rate in a typical storage ring. Thus, the price for obtaining subpicosecond pulses in a storage ring is a significant loss in the average flux and brightness of the source. Another reason for the small flux comes also from the incoherent nature of the electron emission resulting in a condition when the peak power of the radiation is proportional to the peak electron current. A substantial gain in photon flux is reached with Free Electron Lasers (FELs) [15, 21–23] thanks to the coherent nature of the emission when the peak power of the radiation is proportional to the square of the peak electron current due to microbunching of the electrons. Compared to the SASE (Self Amplified Spontaneous Emission) FELs that are currently under operation [23–25], seeded FELs have better temporal and spectral properties [26]. Since microbunching in the seeded FEL originates due to the electron beam interaction with an external laser, they are also easier to use for pump-probe experiments due to intrinsic synchronization with the pump laser. The implementation of seeded FELs in storage rings has been demonstrated in the VUV range and below [27–30]. However, both in storage ring and in FELs, limitations arise at shorter wavelengths because of low microbunching efficiency at the high harmonic of the laser frequency. Recently the proposed new seeding technique called Echo-Enabled Harmonic Generation (EEHG) [31, 32] significantly improves efficiency for a microbunching of electrons at a high harmonic of the seeding laser. A proof-of-principle experiment has been also carried out [33].

In this letter, we propose to join EEHG with the storage ring and enable Coherent Synchrotron Radiation (CSR) in the soft x-ray region with the goal of obtaining higher photon flux within subpicosecond x-ray pulses compared to a "slicing" source. We expect that in addition to the enhanced intensity, the subpicosecond x-ray CSR source will possess substantially improved temporal coherence and a larger signal-to-noise ratio. After a description of the process, we analyze how coherent radiation can be achieved in the x-ray domain using the SOLEIL storage ring as a specific case.

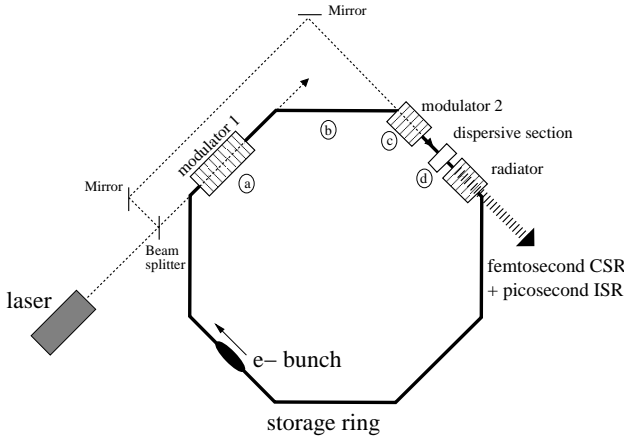


FIG. 1: Proposed scheme layout. a) first laser electron interaction in modulator 1, b) transport of the electrons through part of the storage ring, c) second laser interaction in modulator 2, d) passage of the electrons through an adaptive dispersive section and the radiator, where they emit synchrotron radiation. The two laser pulses can be provided by the same oscillator (as in this figure), or by two synchronized oscillators.

Figure 1 presents the proposed scheme. In addition to the usual production of synchrotron radiation in a third generation light source, it includes two additional laser/electron interactions and an adaptive dispersive section.

The electron bunch evolution starts from a Gaussian distribution along the transverse directions  $x, x', y, y'$  and along  $p$ , the energy difference with respect to electron beam energy  $E_0$  normalized to the RMS energy spread  $\sigma_E$ . Since the electron bunch is much longer than the fs laser pulse, the electron bunch distribution  $f$  can be considered as uniform along the longitudinal coordinate  $z$  (taken in meters), i.e.,

$$f(x, x', y, y', p) = N e^{-\frac{1}{2} \left( \left( \frac{x}{\sigma_x} \right)^2 + \left( \frac{x'}{\sigma_{x'}} \right)^2 + \left( \frac{y}{\sigma_y} \right)^2 + \left( \frac{y'}{\sigma_{y'}} \right)^2 + p^2 \right)} \frac{1}{(2\pi)^{5/2} \sigma_x \sigma_{x'} \sigma_y \sigma_{y'}},$$

with  $N$  being the number of electrons per unit of length of the beam. Table I shows the change of coordinates taking place along the different steps and Figure 2 illustrates the electron bunch distributions in the longitudinal phase space using SOLEIL [20] parameters (see Table II). The first laser/electron interaction in the first undulator called modulator 1 (step a) leads to a modulation of amplitude  $A_1$  (in units of  $\sigma_E$ ) of the electron energy at the laser wavelength  $\lambda_L$  in a length of the order of one  $\sigma_{L1} \times c$  with  $c$  the light velocity (Fig. 2a,a').

The laser pulse of waist  $w_1$  is transversely centered on the electron bunch center. Then, the electron bunch travels in a storage ring section where it experiences dispersion (step b): as the path taken by electrons depends on their energy, the induced laser energy modulation drifts in the longitudinal direction (Fig. 2b,b'), and usually in the transverse directions (the dispersion strengths are characterized by the transfer matrix coefficients  $R_{ij}^{(1)}$  with  $i, j = 1, 2, 3, 4, 5, 6$ ). However the structure after the transport (Fig. 2b') appears only if the optics is configured such that the transverse dispersion between the two modulators is zero or very weak ( $R_{51}^{(1)} \simeq R_{52}^{(1)} \simeq 0$ ). Thus, from symmetric considerations ( $R_{16}^{(1)} \simeq R_{26}^{(1)} \simeq 0$ ), the fs energy modulated electrons cannot be separated transversely from the picosecond electron bunch, like in the slicing scheme [16]. The longitudinal dispersion ( $R_{56}^{(1)}$ ) should not be too strong to prevent the fine structure to be destroyed by the energy fluctuations of amplitude  $\Delta\sigma_E$  introduced by Incoherent Synchrotron Radiation (ISR) in bending magnets ( $\Delta\sigma_E^2 = \frac{55\alpha(\hbar c)^2}{48\sqrt{3}} \frac{L}{R^3} \gamma^7$ , with  $\alpha$  the fine structure constant,  $\hbar$  the Planck constant,  $\gamma = E_0/m_0c^2$  the normalized energy,  $m_0$  the electron mass and  $L$  and  $R$  the length and the radius of the bending magnet, respectively [34]). In the SOLEIL case, the transverse dispersion is cancelled using a Chasman-Green lattice, and the longitudinal dispersion is decreased using an optimized additional chicane system. Then, in step c, the electrons are resubmitted to a second laser of waist  $w_2$ , which again modulates the electron energy at the laser wavelength  $\lambda_L$  (Fig 2c,c'). Just after the second modulator (step d), the

Table I. Coordinate changes at each step of the proposed scheme

<b>Step a</b>	$p = p + A_1 \times e^{-\frac{z^2}{2(c\sigma_{L1})^2}} \cos\left(\frac{2\pi}{\lambda_L} z\right) \times e^{-\frac{x^2+y^2}{w_1^2}}$
<b>Step b</b>	$z \simeq z + p \times R_{56}^{(1)} \frac{\sigma_E}{E_0}$
<b>Step c</b>	$p = p + A_2 \times e^{-\frac{z^2}{2(c\sigma_{L2})^2}} \cos\left(\frac{2\pi}{\lambda_L} z\right) \times e^{-\frac{x^2+y^2}{w_2^2}}$
<b>Step d</b>	$z \simeq z + p \times R_{56}^{(2)} \frac{\sigma_E}{E_0}$

electron bunch passes through an adaptive dispersive section with a longitudinal dispersive strength of  $R_{56}^{(2)}$  (Fig. 2d,d'). With a proper set of parameters, the longitudinal charge distribution  $\rho(z)$  of the electron distribution  $f$  (with  $\rho(z) = \int_{-\infty}^{+\infty} \int_{-\infty}^{+\infty} \int_{-\infty}^{+\infty} \int_{-\infty}^{+\infty} \int_{-\infty}^{+\infty} f(x, x', y, y', z, p) dx dx' dy dy' dp$ ) is modulated at a harmonic  $k$  of the laser wavelength along the overlap of the two laser pulses [31, 32]. The second laser pulse length  $\sigma_{L2}$  is chosen quasi-uniform at the  $\sigma_{L1}$  scale to provide a good bunching all along  $\sigma_{L1}$ . Thus, these so-called "bunched electrons" can emit in phase in the tuned radiator and produce CSR at a harmonic number of the laser wavelength ( $\lambda_r = \lambda_L/k$ ), with a duration near the first laser pulse duration, that is typically 100 fs FWHM. The very weak transverse dispersion should permit to get shorter pulse duration compared to the slicing scheme. Finally, the laser repetition period should be enough long to permit the laser-induced increased of energy spread to be suppressed by synchrotron radiation damping, for a next efficient microbunching creation.

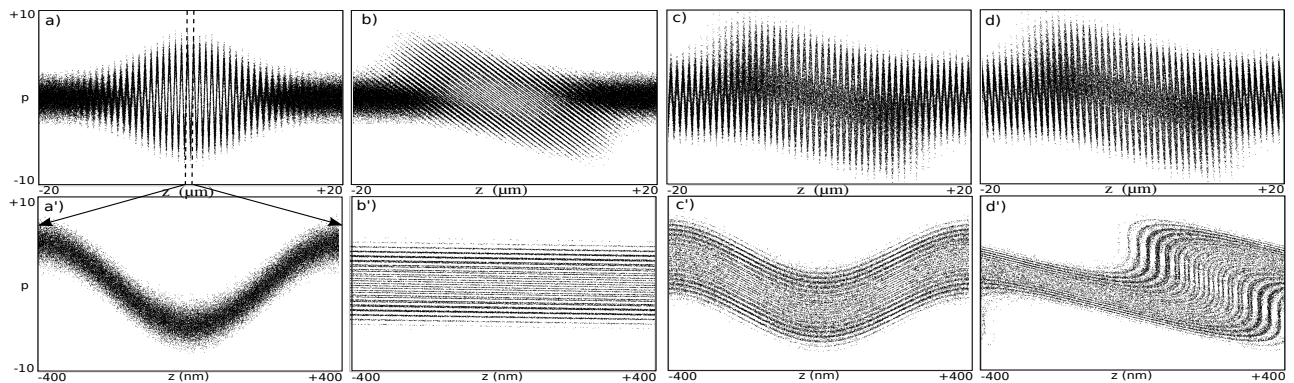


FIG. 2: Calculated electron bunch density in the longitudinal phase space ( $z, p$ ), using a linear 6D macroparticle code including noise from ISR, (a, b, c, d: at the scale of the laser pulse lengths and a', b', c', d': at the scale of the laser wavelength), after the first laser interaction (a, a'), after the first dispersive section (b, b'), after the second laser interaction (c, c') and after the second dispersive section (d, d'). Parameters:  $A_1 = -5$ ,  $A_2 = -2.95$ ,  $R_{56}^{(1)} = -1.5$  mm,  $R_{56}^{(2)} = -48$   $\mu$ m,  $\sigma_{L1} = 21$  fs,  $\sigma_{L2} = 118$  fs,  $w_1 = w_2 = 600$   $\mu$ m ( $A_2$  and  $R_{56}^{(2)}$  chosen to optimize the bunching factor of the thirtieth harmonic). For the figure clarity, some parameter values are different from those in Table II.

Table II. SOLEIL parameters used in our study

Nominal energy $E_0$ (GeV), energy spread $\sigma_E$ (MeV)	2.75, 2.79
Bunch dimensions $\sigma_z$ (mm), $\sigma_x$ ( $\mu$ m), $\sigma_{x'}$ ( $\mu$ rad)	10.5, 147, 33
Bunch dimensions $\sigma_y$ ( $\mu$ m), $\sigma_{y'}$ ( $\mu$ rad)	10.0, 4.8
Peak current $I_{\text{peak}}$ (A)	134
Radius $R$ (m) and length $L$ (m) of a bending magnet	5.39, 1
Chicane length (m) and field (T)	0.65, 0.7
Modulator 1&2 period length (mm)	150
Modulator 1&2 number of periods	13
Radiator period length $\lambda_u$ (mm)	80
Radiator number of periods $N_u$	19
Laser wavelength $\lambda_L$ (nm)	800
Maximum energy laser pulse (mJ)	5
RMS laser pulse length $\sigma_{L1}$ (fs), $\sigma_{L2}$ (fs)	43, 118

We now investigate down to which harmonic number of the laser wavelength the CSR is produced in the SOLEIL case [20]. The radiator of Figure 1 corresponds to an undulator of the TEMPO beamline [20], covering 27.6–0.8 nm, corresponding to a harmonic number  $k$  of the 800 nm Ti:Sa laser wavelength between 29 and 967. The CSR on the  $k^{\text{th}}$  harmonic results in the bunching factor  $b(k)$  defined as  $b(k) = \frac{1}{N} | \langle \rho(z) e^{ikz} \rangle |$  with  $\langle \rangle$  the average along the  $z$  direction. For two laser-electron interactions, an optimized  $b(k)$  can be expressed, for infinite laser pulse length and without transverse dependency, as [32]:

$$b(k) = \left| J_{k+1} [kA_2B_2] J_1 [A_1(B_1 - kB_2)] \times e^{-\frac{1}{2}[B_1 - kB_2]^2} \right|, \quad (1)$$

with  $B_i = R_{56}^{(i)} \frac{2\pi}{\lambda_L} \sigma_E / E_0$  ( $i=1,2$ ) and  $J_k$  the Bessel function of order  $k$ . Further optimization of equation (1) leads to the simpler expression  $b(k) \simeq 0.39 \times k^{-1/3}$  [32], which provides an upper value of the bunching factor versus harmonic number, as shown in Figure 3. This figure also shows

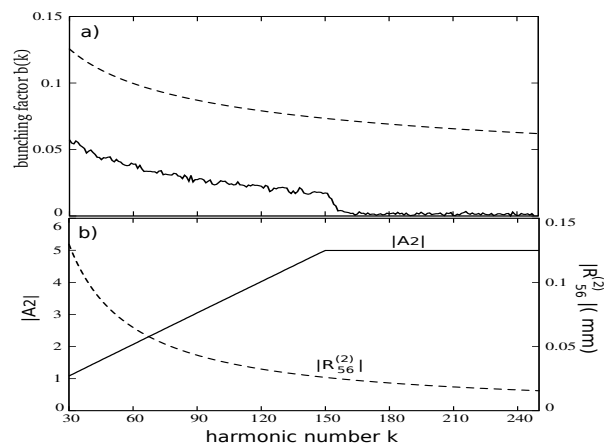


FIG. 3: a) – Bunching factor  $b(k)$  just before the radiator versus the harmonic number  $k$  (calculated with a linear 6D macroparticle code over one laser wavelength) with  $R_{56}^{(1)} = -4$  mm and  $A_1 = -5$ , and  $- - b(k) = 0.39 \times k^{-1/3}$ . b) associated  $- A_2$  and  $- - R_{56}^{(2)}$ .

the reduction of  $b(k)$  (calculated with a 6D linear macroparticle code) considering (i) the transverse dynamics, (ii) the noise induced by ISR [32], (iii) the finite laser pulse dimensions  $\sigma_{L1}$ ,  $\sigma_{L2}$ ,  $w_1$ ,  $w_2$  and (iv) a limitation imposed on the amplitude of the second energy modulation  $A_2$ , i.e., of  $5 \sigma_E$  in the SOLEIL case (with a laser pulse energy of 5 mJ,  $w_2 = 600$   $\mu$ m and  $\sigma_{L2} = 118$  fs [35]). The bunching factor decreases smoothly with  $k$  towards a cut-off corresponding to  $|A_2|$  reaching the limit value of 5 (Fig. 3b). The position of the cut-off strongly depends on the  $R_{56}^{(1)}$  value and is of  $k \simeq 150$  ( $\lambda_r \simeq 5.3$  nm) for  $R_{56}^{(1)} = -4$  mm. Associated values of  $A_2$  and  $R_{56}^{(2)}$  (Fig. 3b) have been chosen from Eq. (1), and the absolute value of  $A_1$  is taken as 5 since a saturation of the bunching factor arises at about this value [32]. First studies taking into account non-linear terms in the transport indicate that the structure can still be preserved.

In order to analyze the enhancement of the emitted power with respect to the slicing scheme, the CSR peak power  $P_{CSR}$  is estimated with an analytical formula taken from [36] and further modified to take into account  $\sigma_{x'}$ ,  $\sigma_y$ ,  $\sigma_{y'}$  and the transverse incoherent part of the radiation:

$$P_{CSR} = \pi\alpha\hbar\omega \frac{K^2}{1 + K^2/2} [JJ]^2 \frac{I_{\text{peak}}}{e} n_e b^2 \sqrt{f_2}, \quad (2)$$

with  $n_e = \frac{I_{\text{peak}}\lambda_r N_u}{ce}$  the number of electrons within the slippage length  $\lambda_r N_u$ ,  $N_u$  the radiator period number,  $f_2 = (\sigma_r \sigma_{r'})^2 / (\sqrt{\sigma_r^2 + \sigma_x^2} \sqrt{\sigma_{r'}^2 + \sigma_{x'}^2} \sqrt{\sigma_r^2 + \sigma_y^2} \sqrt{\sigma_{r'}^2 + \sigma_{y'}^2})$ ,  $\sigma_r = \sqrt{2\lambda_r \lambda_u N_u} / 4\pi$  and  $\sigma_{r'} = \sqrt{\lambda_r / 2\lambda_u N_u}$ , respectively, the RMS size and divergence of the undulator fundamental mode,  $\omega = 2\pi c / \lambda_r$ ,  $e$  the electron charge,  $K = \sqrt{4\lambda_r \gamma^2 / \lambda_u - 2}$ ,  $[JJ] = [J_0(x) - J_1(x)]$  and  $x = \frac{K^2}{4 + 2K^2}$ . At  $k = 30$  ( $\lambda_r = 26.7$  nm) with  $b = 0.05$  (Fig. 3a),  $P_{CSR} \simeq 187$  kW.

We also calculate the CSR peak power  $P'_{CSR}$  with GENESIS [37] along one laser wavelength with the previously optimized parameters, as shown in Figure 4. The second laser peak power and the  $R_{56}^{(2)}$  values are further adjusted to obtain a bunching factor around 5%. The output power  $P'_{CSR}$  is about 120 kW, a value in good agreement with the one found with Eq. (2).

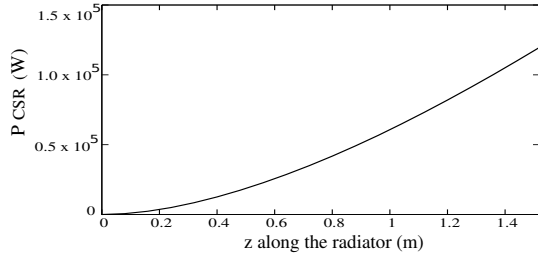


FIG. 4: Emitted power along the radiator at 26.7 nm (30<sup>th</sup> harmonic of the laser wavelength). Output power:  $P'_{CSR} \simeq 1.2 \times 10^5$  W. Parameters: first (resp. second) laser peak power=8 GW (0.8 GW), waist of the two lasers : 0.6 mm,  $R_{56}^{(1)} = 4$  mm,  $R_{56}^{(2)} = 120$   $\mu$ m.

In comparison, the power in the usual slicing case  $P_{ISR}$ , given by  $P_{ISR} = \dot{N}_{\text{phot}} \hbar\omega \times \eta$  is of 0.135 W at  $\lambda_r = 26.7$  nm and for the planned relative bandwidth  $\Delta\omega/\omega$  value of 0.05% (with  $\eta$  the percentage of electrons involved in the fs light pulse, typically  $\eta = 0.1$  and  $\dot{N}_{\text{ph}}(\omega) = \pi\alpha N_u \frac{\Delta\omega}{\omega} \frac{I_{\text{peak}}}{e} \frac{K^2 [JJ]^2}{1 + K^2/2}$  [34]). The power is increased by about 6 orders of magnitude with the two laser-electron interactions. The signal-to-noise ratio  $S/N$ , i.e., the fs CSR energy emitted by the bunched electrons compared to the picosecond ISR energy emitted by all the electrons in the bunch is  $S/N = \frac{P_{CSR} \times \sigma_{L1} \eta c}{P_{ISR} \times \sigma_z} = \frac{n_e b^2 \sqrt{f_2} \sigma_{L1} c}{\sigma_z} N_u \frac{\Delta\omega}{\omega} \simeq 168$  (or  $S'/N = \frac{P'_{CSR} \times \sigma_{L1} \eta c}{P_{ISR} \times \sigma_z} \simeq 110$ ), assuming a CSR Gaussian emission. Finally, we notice that with the planned value of  $\Delta\omega/\omega$ , experimentally adjusted using a monochromator,

all the CSR can be collected assuming a Fourier-transform-limited pulse, whereas a large part of the ISR is suppressed.

In summary, we proposed a mechanism for producing femtosecond coherent synchrotron radiation in the soft x-ray region in storage rings using two electron-laser interactions (an echo scheme). For the SOLEIL case presented here, for which practical design issues were addressed, the CSR extends down to 5 nm and provides about 150 kW at 27 nm, which is 6 orders of magnitude higher than the power obtained under the same conditions with the slicing scheme. The extension of CSR towards shorter wavelengths could be achieved with a lower beam energy and shorter laser wavelengths.

The authors acknowledge M. Labat, S. Reiche and G. Stupakov for helpful discussions. Also AZ acknowledges DoE Contract No. DE-AC02-06CH11357.

- 
- [1] A. H. Zewail, J. Phys. Chem. A **104**, 5660 (2000).
  - [2] K. Sokolowski-Tinten et al., Nature **422**, 287 (2003).
  - [3] D. M. Fritz et al., Science **315**, 633 (2007).
  - [4] S. L. Johnson et al., Phys. Rev. Lett. **100**, 155501 (2008).
  - [5] C. Rischel et al., Nature **390**, 490 (1997).
  - [6] C. Bressler and M. Chergui, Chem. Rev. **104**, 1781 (2004).
  - [7] A. Cavalleri et al., Phys. Rev. Lett. **95**, 067405 (2005).
  - [8] C. Stamm et al., Nat. Mater. **6**, 740 (2007).
  - [9] C. Bressler et al., Science **323**, 489 (2009).
  - [10] L. X. Chen et al., J. Phys. Chem. B **103**, 3270 (1999).
  - [11] P. o. Salières, Phys. Rev. Lett. **74**, 3776 (1995).
  - [12] I. McKinnie and H. Kapteyn, Nat. Photon. **4**, 149 (2010).
  - [13] M. M. Murnane et al., Science **251**, 531 (1991).
  - [14] F. Zamponi et al., Appl. Phys. A **96**, 51 (2009).
  - [15] M.-E. Couprie and J.-M. Filhol, C. R. Physique **9** (2008).
  - [16] A. A. Zholents and M. S. Zolotarev, Phys. Rev. Lett. **76**, 912 (1996).
  - [17] W. Schoenlein et al., Science **287**, 2237 (2000).
  - [18] S. Khan et al., Phys. Rev. Lett. **97**, 074801 (2006).
  - [19] P. Beaud et al., Phys. Rev. Lett. **99**, 174801 (2007).
  - [20] A. Nadji et al., IPAC'10 p. 2499 (2010).
  - [21] A. Kondratenko and E. Saldin, Part. Acc. **10**, 207 (1980).
  - [22] K.-J. Kim, Phys. Rev. Lett. **57**, 1871 (1986).
  - [23] P. Emma et al., Nature Photonics **4**, 641 (2010).
  - [24] W. Ackermann et al., Nature Photonics **1**, 336 (2007).
  - [25] T. Shintake et al., Phys. Rev. ST Accel. Beams **12**, 070701 (2009).
  - [26] L.-H. Yu et al., Science **289**, 932 (2000).
  - [27] R. Prazeres et al., Nucl. Instrum. Methods A **304**, 72 (1991).
  - [28] G. De Ninno et al., Phys. Rev. Lett. **101**, 053902 (2008).
  - [29] T. Tanikawa et al., FEL'09 p. 285 (2009).
  - [30] V. N. Litvinenko, Nucl. Instrum. Methods A **507**, 265 (2003).
  - [31] G. Stupakov, Phys. Rev. Lett. **102**, 074801 (2009).
  - [32] D. Xiang and G. Stupakov, Phys. Rev. ST Accel. Beams **12**, 080701 (2009).
  - [33] D. Xiang et al., Phys. Rev. Lett. **105**, 114801 (2010).
  - [34] A. W. Chao and M. Tigner, Handbook of Accelerator Physics and Engineering (World Scientific, 2006).
  - [35] A. A. Zholents and K. Holldack, FEL'06 p. 725 (2006).
  - [36] Z. Huang and K.-J. Kim, PAC'99 p. 2495 (1999).
  - [37] S. Reiche, Nucl. Inst. Meth. A **429**, 243 (1999).